

## Durability and wear of engine parts – new methods of testing of alloys and composites

Zbigniew Ranachowski<sup>1</sup>, Andrzej Pawełek<sup>2</sup>, Zdzisław Jasieński<sup>2</sup>, Andrzej Piątkowski<sup>2</sup>  
Stanisław Kudela Jr.<sup>3</sup>, Marcin Lewandowski<sup>1</sup>, Paweł Mazuruk<sup>4</sup>

<sup>1</sup> PAS, Institute of Fundamental Technological Problems  
02-106 Warszawa, ul. Pawińskiego 5 B, e-mail: zranach@ippt.pan.pl

<sup>2</sup> PAS, Institute of Metalurgy and Materials Engineering  
30-059 Kraków, ul. Reymonta 25

<sup>3</sup> Slovak Academy of Sciences, Institute of Materials and Machine Mechanics  
830-08 Bratislava, Račianska 75, P.O. box 95, Slovakia

<sup>4</sup> BU Power Systems Polska  
02-293 Warszawa, ul. Krótka 6

**Key words:** Diesel engines diagnostics, light alloys and composites, Common Rail fuel system, Acoustic Emission method

### Abstract

The paper deals with the problems related to the diagnostics of selected parts of modern Diesel engines. The evolution of mechanical properties of four alloys of Mg-Li-Al system and four composites made on the base of the alloys mentioned above, caused by variation of its composition was presented. The Acoustic Emission (AE) method applied to monitoring of degradation of mechanical properties of the alloys and composites was described. Moreover, the results of the investigation of failures occurring in the injectors of Common Rail Diesel engines performed with the application of AE method were also reported.

### Introduction

Diesel engines serving as the main and auxiliary propulsion of different vessels and vehicles are objects of permanent improvements. The engines with Common Rail (CR) fuel system were introduced to comply with new strict environmental regulations dealing with limits of emissions of: carbon oxide, hydrocarbons, nitrogen oxides and particulate pollutants. The CR Diesel engines controlled by sophisticated electronic systems and sensors are characterised by high (> 50%) efficiency and increased reliability. Operating with different way than those of mechanical fuel supply controlling, the CR system engines suffer from specific fault types. The novel method of non-invasion method of diagnostic of the faults mentioned above will be described below. The other important problem of development of engines is the choice of the light and durable materials to construct them. As far as now, Diesel engines suffer from the relative high (0.5–2

kg/kW) mass related to power unit. Gravity reduction causing no negative impact on reliability would create economic gains and cause the further technological progress. As an example of the importance of the matter the results achieved by the engineers of the Cassidian Company being a corporate of EADS can be recalled here. Cassidian has introduced a sort of Unmanned Aerial Vehicle (UAV) designed to be a surveillance and imaginary platform for naval and rescue purposes. Having 300 kg of weight UAV, called Tanan 300, is able to carry a 50 kg payload, including an AIS (Automatic Identification System), an IFF (Identification Friend or Foe) system, maritime radar, an electronic HD surveillance system, and a direction finder. The aircraft's endurance is quoted at eight hours at the flight speed of 100 km/h. To meet these difficult requirements the designers have chosen a lightweight Diesel engine to drive it as the optimal solution. It is highly probable that other autonomous boats/vehicles would be soon in service.

The image of the Tanan 300 helicopter on the basis of the data taken from the website of Cassidian company is shown in the figure 1.



Fig. 1. The image of the remote-controlled Tanan 300 helicopter. The lightweight Diesel engine is applied to drive the machine [the advertisement of the Cassidian company at [www.miltechmag.com/2012/08/cassidians-tanan-300-vtol-uas.html](http://www.miltechmag.com/2012/08/cassidians-tanan-300-vtol-uas.html)]

### Testing of lightweight alloys and composites

The comparison of the mechanical properties of the engineering materials can be done by recalling of their parameters – yield strength (YS) and tensile strength (TS). These parameters can be applied in the assessment of the sustained load possible to withstand for the element made of the considered material. The low grain and properly tempered steel of good quality achieves ca. 400 MPa of TS. Its specific gravity is remarkable and equals ca. 7900 kg/m<sup>3</sup>. Therefore, nowadays lightweight alloys of system of Mg-Al or Mg-Al-Li, are applied as parts of engines. After the proper processing these alloys have TS close to 200 MPa, but they are considerably lighter than steel with the specific gravity of 2000 kg/m<sup>3</sup>. The alternate way of improving of the mechanical strength of the engine part is to replace the alloy with the composite. The example of the composite can be the material which base material (matrix) is a lightweight alloy and it is reinforced by immersion of high strength ceramic fibres acting as the skeleton.

The authors of the paper have compared the mechanical properties of four lightweight Mg-Li-Al system alloys and of four composites made on their base. The authors have used relatively small specimens for testing (i.e. the 10×10×10 mm cubes) and therefore application of the tensile stress was of no use. Instead the specimens were compressed what enabled for the determination of the yield strength changes caused by the modification of material composition. The Mg9Li, Mg9Li1Al, Mg9Li3Al and Mg9Li5Al alloys are build of two material

phases. The mechanical properties of the  $\alpha$  phase are worse than these of the  $\beta$  phase compensated by considerably higher plasticity, very good machine and weld abilities. Adding of aluminium causes additional expansion/compression strengthening but in practical applications the excess of Al may result in the loss of the necessary ductility. Figure 2 presents the results of the measurements of the compressing stress of investigated lightweight alloys.

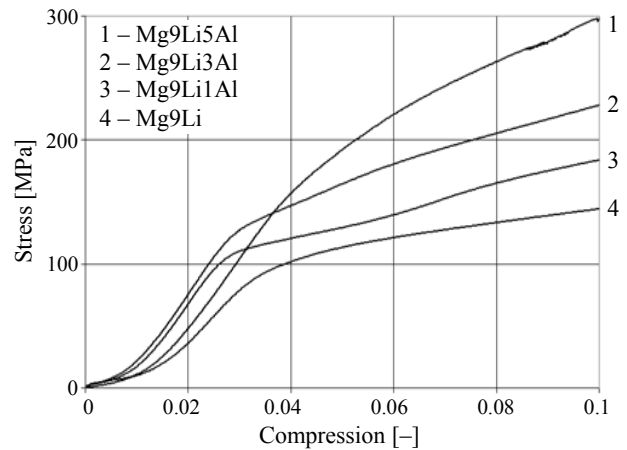


Fig. 2. The dependence stress versus compression measured in lightweight alloys with different amount of Al admixture

Analysing the data presented in figure 2 one can note that the YS and also possible range of the applicable stresses does not exceed 140 MPa. It increases according to the increasing admixture of Al. Composites based on Mg-Li and Mg-Li-Al alloys were prepared in cooperation with the Institute of Materials and Machine Mechanics of the Slovak Academy of Sciences, Bratislava. They were produced from a fibrous skeleton of commercial Saffil – subjected to infiltration under pressure in a bath of liquid alloy in a laboratory autoclave. Their length oscillated from 100 to 500  $\mu\text{m}$ , and the mean size of the diameter was 3÷4  $\mu\text{m}$ . They were characterised by high tensile strength of 1.5 GPa and the melting point exceeding 2000 Centigrade. The optimal contribution to the alloy was 10% by weight.

Figure 3 presents the dependence stress versus compression measured in composites made of lightweight alloys with different amount of Al admixture and reinforced with Saffil fibres.

The experimental results shown in figure 3 let the authors to conclude that the composites made in the basis of Mg9Li1Al, Mg9Li3Al and Mg9Li5Al alloys present the similar strength and YS, regardless on the amount of Al admixture. Their YS is remarkably higher than that determined in the alloys being the matrix of the material, which is ca.

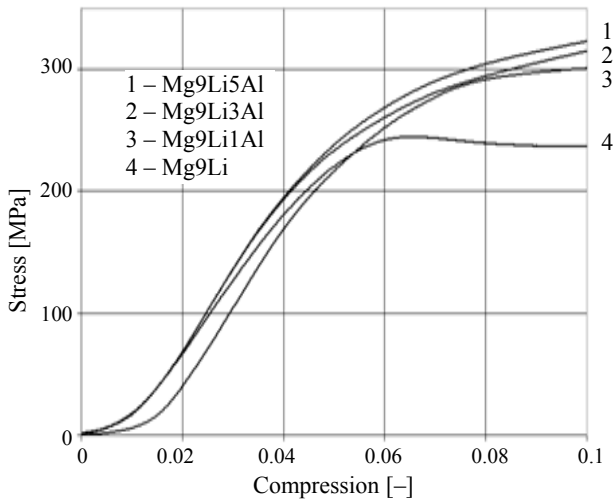


Fig. 3. The dependence stress versus compression measured in composites made of lightweight alloys with different amount of Al admixture and reinforced with Saffil fibres, 10% by weight

200 MPa. Therefore, there is possibility of application of the investigated composites to become parts of lightweight engines. It should be noted that the development of destruction mechanisms in overloaded composites is different than that appearing in alloys. In the latter materials the plastic deformation is related with the onset of the evolution of large dislocation systems and also with the crack growth initiated by the presence of voids and structural defects. In the composites being the object of present investigation the mechanical stress is taken over by the fibrous skeleton rather than by the ductile alloy. The collapse of the system appears when the majority of the fibres is broken or pulled out of the matrix. That process is undergoing with complex, partly fragile and partly plastic stages. This is a reason that for the research during the mechanical loading of composite elements the Acoustic Emission (AE) signal is registered [1]. The origin of this signal is a structural degradation of the tested object. The authors of the paper have registered the AE signal during compression tests of the specimens described above. A standard instrumentation, schematically shown in figure 4 was used in this purpose.

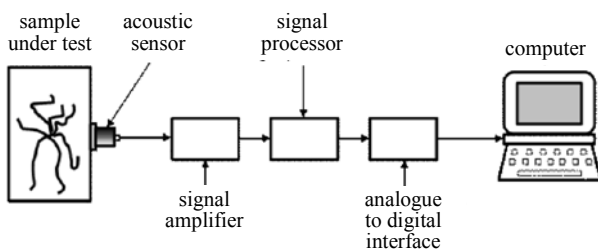


Fig. 4. Block – diagram of the instrumentation for registration of AE signal generated during compression tests of alloys of Mg-Li-Al system and composites made on their base

During the compression of the alloys of Mg-Li-Al system the maximum energy of AE signal is evoked by the activated dislocation systems when a yield limit of the material is reached. In the composites the AE activity is registered in wider range of compression and it is caused by the local breaking of the mechanical durability by the rigid fibrous skeleton. At this moment the fibres are breaking or pulling out of the matrix. Later there appears the relaxation of the alloy and this causes the stress redistribution among the next parts of the skeleton. In figure 5 the comparison of the AE signal generated when the Mg9Li1Al alloy and a composite made on its base are compressed in similar process. The next figure 6 presents the result of a specific processing of AE signal generated during the breaking of the composite fibres. The composite was compressed until the reach of linear compression level 0.05. The image has a form of a spectrogram where two-dimensional projection of signal processing is applied. The horizontal axis represents the time flow in seconds and the vertical axis represents a generated signal frequency in Hertz. The AE pulses generated during the skeleton breaks are visualised as a thin red lines. The spectrograms of the processes evoking the AE signals are used mostly in the purpose to identify the signal origins of different spectral signature operating simultaneously.

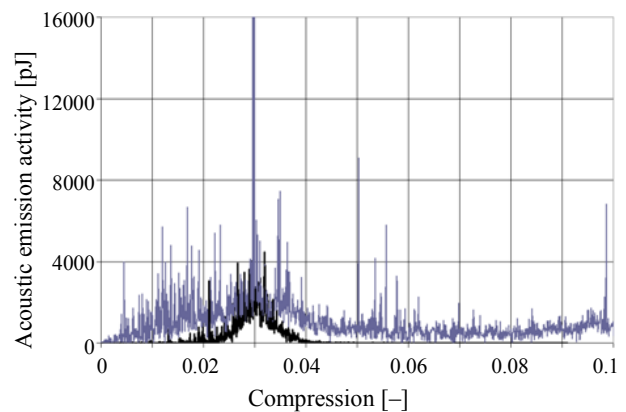


Fig. 5. Time dependence of AE signal energy generated in compressed specimen of Mg9Li1Al alloy (black line) and in compressed in the same way Mg9Li1Al alloy based composite (grey line)

The comparison of the mechanical properties of the loaded construction elements and also monitoring of the stages of their degradation is possible with the use of AE method. The authors of the paper have performed such investigation in different compositions of alloys of Mg-Li-Al system and in composites reinforced with Saffil and carbon fibres. The tests were performed at room and at elevated

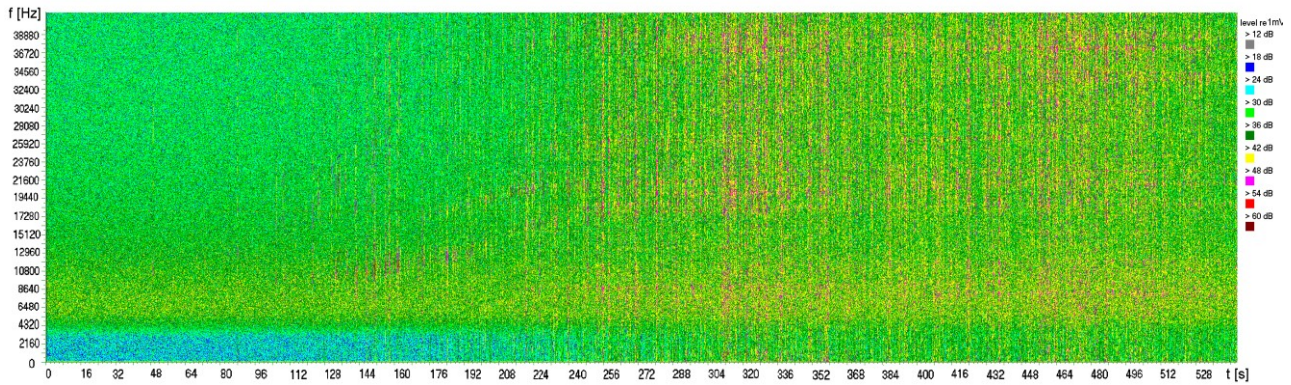


Fig. 6. Two axial frequency – time projection of the fibre breaking process of the composite shown in figure 5. The AE pulses generated during the fibre breaks are visualised as a thin red lines

temperature (150°C). The results were published in [2, 3, 4, 5].

### Investigation of Common Rail fuel system faults

After the longer period of servicing Diesel engines with Common Rail fuel system – what was his professional occupation – one of the authors of the paper has created the ranking of faults affecting these engines. To the most frequent one can include: fuel system faults (70%), faults of controllers (11%), crankshaft faults (4%). The superiority of the first enlisted damage type results from the circumstance that the proper operation of the fuel system relies on the quality of precise collaborating parts working at high pressures and under high capacity impacts of short duration. Small mechanical impairments appearing in collaborating parts of the fuel dosage sections of CR injectors result in pressure drop in high-pressure supply rail what causes the start up of the engine unworkable. The common fault of the CR fuel system is the damage of the electromagnetic injector dosage control valve. This fault results in excess fuel outflow to the outlet line and therefore the pressure drop in high-pressure supply rail. There is no confirmation that the fault is caused by natural wear of the injector elements because the faults were recognised either after several hundreds or after several tens of engine operation hours. To solve the problem a special diagnostic procedure was developed to identify the damaged injector during its operation in running engine [6, 7]. The authors of the paper have performed their investigation on industrial four-lined cylinder Perkins engine of 102 kW power at 2200 rev/min.

A special tool to identify and complete the population of the injectors with abnormal outflow was designed. The tool enables to determine the

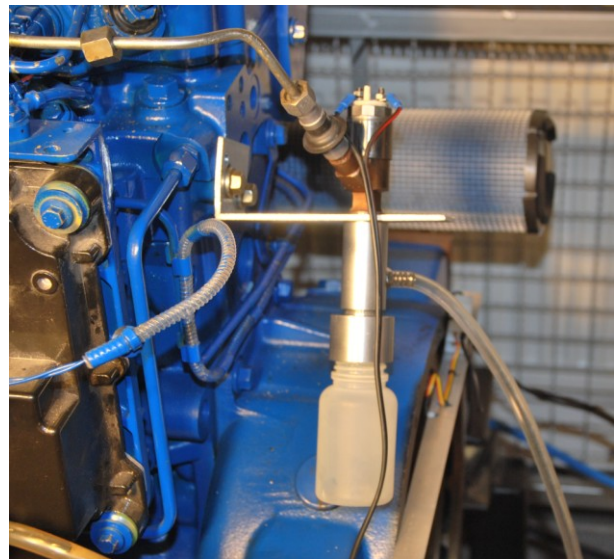


Fig. 7. A tool to identify the injectors with abnormal outflow designed by one author of the paper

amount of fuel leaving the injector to the outlet line and its view is presented in figure 7.

The tool mentioned above consists of two parts with O-rings between them. The injector body is covered by the upper part of the tool. This part includes the fuel container connected to the fuel outlet with the stub. During the operation of the injector it produces the fuel outflow what is transferred to the fuel container. Then it travels further on to the measuring cylinder via the outlet line. The lower part of the tool gathers the fuel streaming from the atomizer. The injector under test is supplied by the electric current supply and high-pressure line originally leading to the one of the cylinder of hosting engine. The current supply was matched by custom made interconnector.

The data found in engine documentation let the authors to determine the acceptable amount of the fuel outflow in non-damaged injector to 120 cm<sup>3</sup> per 3 minutes of operation at 1000 rev/min. of low

load. The outflow measurements results performed in a population of 24 injectors are shown in figure 8. The non-damaged injectors are labelled with “N” code and the damaged ones are labelled with the “U” code.

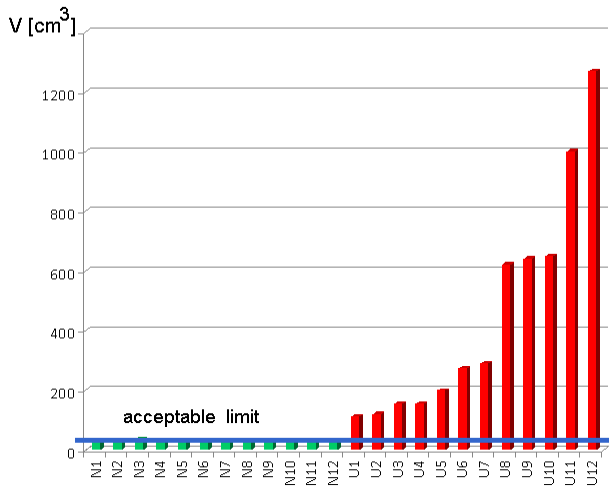


Fig. 8. The outflow measurements results performed in a population of 24 injectors

The outflow measurements were additionally verified using a professional Hartridge IFT-70 system. A part of the injectors, i.e. the specimens No. N1-N12 and U1-U6 were then used to register the Acoustic Emission signal during their operation. The tests were performed with application of modified analyser regarding the schematic presented in figure 4. The analyser used for testing the injectors was a custom made portable type for convenient application at running engines. It was equipped with rechargeable battery supply and a LCD screen housed in a hard metal case. AE signal was processed by a microcontroller of type AT91SAM7 and the half second long data record was stored in a SD type memory card with the possibility of transferring to the laptop computer via USB transmission line. The half second data record consisted of 25,000 signal samples recorded every 20 microsecond to be processed further in the computer. 60 data sets

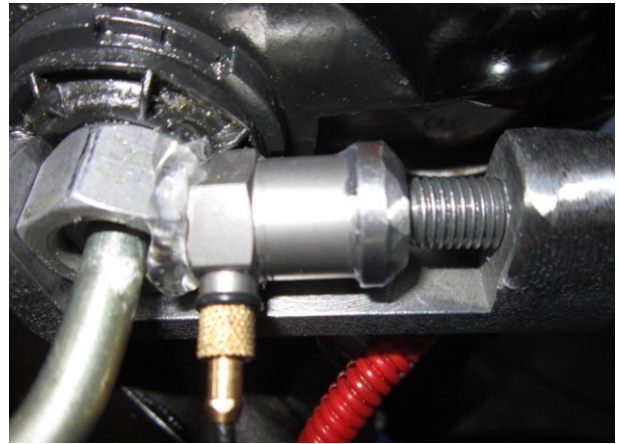


Fig. 9. The AE sensor to matched the tested injector high pressure line stub by a special clamp holder

were picked of every injector under test to perform adequate statistic analysing. The method of matching of the AE sensor to the tested injector is shown in figure 9. Figure 10 present a spectrogram being a result of injector operation at four-cylinder engine. At the spectrogram one can determine the traces of activity of four injectors, however, the tested one produces the signal of higher energy level (red coloured one) because the elements of this injector lie in the vicinity of the sensor. The comparison of the spectrograms derived from the damaged and good injectors did not allow for a damage identification. The reason was an insufficient resolution in time domain of produced images of the signal. To deliver a more precise tool for a signal analysing the authors of the paper have designed a custom made software enabling for determination of characteristic segments of the investigated signal with a 100 microsecond resolution. The time dependence of the registered AE signal and applied current driving a solenoid of injection control valve, projected in high resolution is shown in figure 11.

The signal of EA presented in figure 11 (bright colour) consists of a three pulses whose together last ca. 3 milliseconds. First two leading pulses are

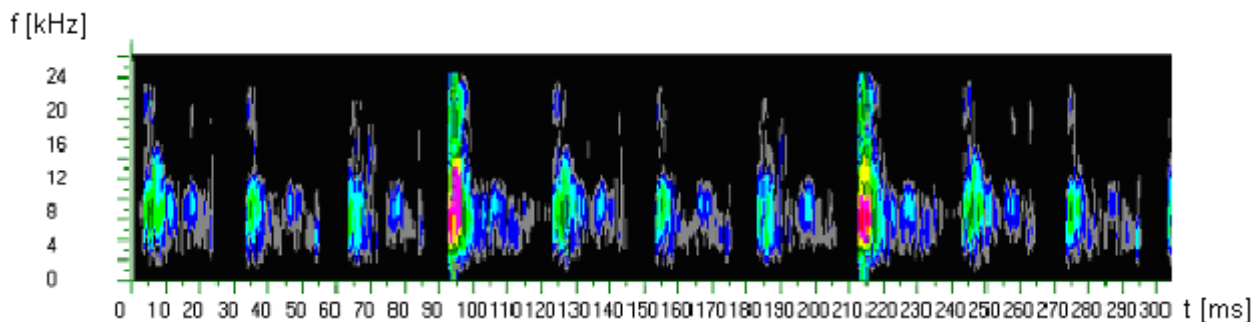


Fig. 10. A spectrogram being a result of injector operation at four cylinder engine. At the spectrogram one can determine the traces of activity of four injectors, however, the tested one produces the signal of higher energy level (red coloured one). This enables for automatic detection of a working injector

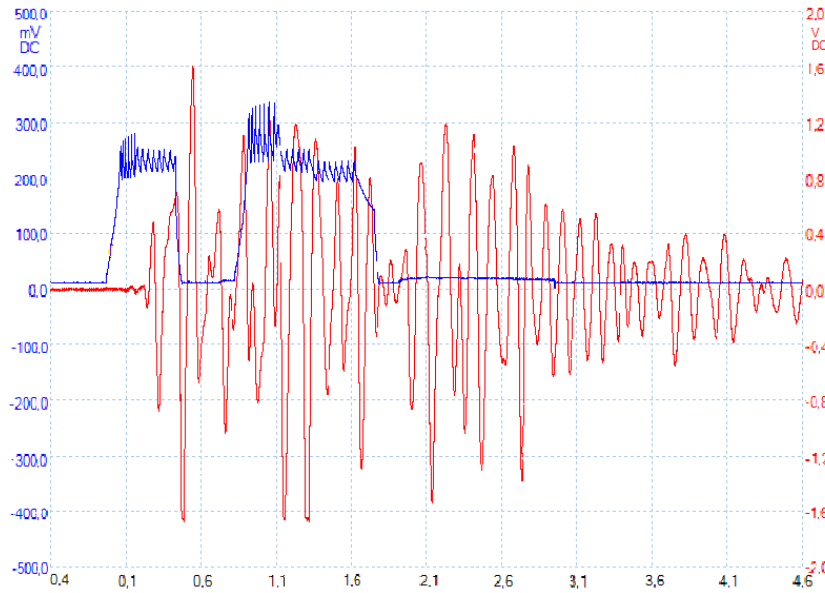


Fig. 11. The time dependence of the registered AE signal and applied current driving a solenoid of injection control valve, projected in high resolution. The time unit presented in horizontal axis is 1 millisecond

caused by the operation of electromagnetic injector dosage control valve. A ca. 0.6 millisecond dead time appears after their completion and then the contact of the injector needle and its bed generates the third pulse lasting ca. 0.8 of millisecond. The digital set of AE signal samples being a record of this process includes 150 elements. A custom made software enabling for determination of characteris-

tic segments delivers the information determining duration of three characteristic phases of the process mentioned above:

- I – electromagnetic injector dosage control valve activity;
- II – dead time during increase of a pressure controlling the operation of injector needle;
- III – injector needle activity causing a fuel spread.

Table 1. The average time duration, standard deviation and relative deviation referred to average duration  $\Delta$  calculated for three phases of injectors activity above for 60 records made in 18 examined items

No.	Injector label	I phase time duration for $k = 60$ tests			II phase time duration for $k = 60$ tests			III phase time duration for $k = 60$ tests		
		$t$ [ms]	Standard deviation $\sigma$	$\Delta$ [%]	$t$ [ms]	Standard deviation $\sigma$	$\Delta$ [%]	$t$ [ms]	Standard deviation $\sigma$	$\Delta$ [%]
1	NN1	0.86	0.07	8.66	0.48	0.31	64.50	0.63	0.16	24.82
2	NN2	1.05	0.16	15.24	0.67	0.60	89.12	0.60	0.14	24.05
3	NN3	0.81	0.04	5.29	1.03	0.78	75.38	0.56	0.13	23.24
4	NN4	0.82	0.05	5.90	0.83	0.30	36.14	0.58	0.14	24.09
5	NN5	1.12	0.14	12.07	0.45	0.26	57.43	0.61	0.19	31.52
6	NN6	1.06	0.11	10.09	0.42	0.20	47.01	0.78	0.17	21.56
7	NN7	1.03	0.18	17.91	0.46	0.75	164.69	0.59	0.13	22.44
8	NN8	1.18	0.15	12.42	0.24	0.29	123.49	0.86	0.20	23.77
9	NN9	0.98	0.10	9.97	0.68	0.50	73.48	0.58	0.17	28.78
10	NN10	1.23	0.20	15.94	0.26	0.22	84.47	0.80	0.29	35.73
11	NN11	0.95	0.07	7.64	0.51	0.39	77.20	0.71	0.26	37.25
12	NN12	0.89	0.08	9.38	0.90	0.64	71.30	0.58	0.16	27.41
13	UU1	0.98	0.26	26.09	0.18	0.43	245.82	0.87	0.42	47.86
14	UU2	0.96	0.14	15.11	0.49	0.55	111.44	0.87	0.43	49.45
15	UU3	0.96	0.21	21.85	0.19	0.39	203.66	0.76	0.34	45.03
16	UU4	0.92	0.20	21.37	0.17	0.29	171.63	0.75	0.35	46.45
17	UU5	0.82	0.04	5.18	0.74	0.77	56.53	0.52	0.07	14.07
18	UU6	0.89	0.16	17.79	0.41	0.60	145.91	0.69	0.31	44.57

The average time duration, standard deviation and relative deviation referred to average duration  $\Delta$  calculated for three phases enlisted above for 60 records made in 18 examined injectors are presented in table 1. The data presented in this table let the authors to conclude that the average duration of the first phase is of no use for a damage / no damage classification of the injectors but the duration of the second and the third phase correlates with the state of the tested element. The workable rule of effective classification is presented then in table 2. The percentage of true and false injector classifications regarding the rule of table 2 and applied to the population of 18 injectors enlisted in table 1 is summarised in table 3. The entire participation of right classifications in this population equals 94% what suggests a possibility of application of the described rule in a practical diagnostics.

Table 2. Damage / no damage classification rule using AE signal from injector operation phase duration

Condition for relative II phase deviation referred to average duration $\Delta$	Condition for relative III phase deviation referred to average duration $\Delta$	Result of subordination to one class: 0 – no damage, 1 – damage
$t$ [ms]	$t$ [ms]	
any	$\leq 14\%$	1
any	$> 14\%$ and $< 38\%$	0
any	$\geq 38\%$	1

Table 3. The percentage of true and false injector classifications regarding the rule of table 2 and applied to experimental results enlisted in table 1

Classification matrix items	Detected items with 0 – no damage	Detected items with 1 – damage	Total
Forecasted test result according to the rule presented in table 2, 0 – no damage	12	1	12
Forecasted test result according to the rule presented in table 2, 1 – damage	0	6	6
Total detected for two states	12	6	18
Percentage of right classification	100%	100%	100%

## Conclusions

Nowadays, Diesel engines are applied in numerous technical applications. This leads to a variety of specific construction modifications and a permanent progress if their performance. The wide spread of servicing engines and a necessity of appropriate retaining of reliability implies the need of improving of the diagnostic methods. The authors of the paper hope that method of non-invasive diagnostic method of testing of mechanical loaded machine elements and of engine operation monitoring using the AE analysing and recording – briefly presented here – shall contribute to the increase of the safety of exploited technical objects.

## Acknowledment

The studies were financially supported by the research projects of the Polish Ministry of Science and Higher Education No N507 056 31/128 and No. N N507 598038 as well as by the research project No. 2/0174/08 of the Grant Agency VEGA of the Slovak Republic.

## References

- GROSSE CH., OHTSU M.: Acoustic Emission Testing. Springer, 2008, DOI: 10.1007/978-3-540-69972-9.
- PAWELEK A., RANACHOWSKI Z., PIĄTKOWSKI A., et al.: Acoustic emission and strain mechanisms during compression at elevated temperature of beta phase Mg-Li-Al composites reinforced with ceramic fibres. Archives of Metallurgy and Materials, 52, 1, 2007, 41–48.
- KUDELA S., PAWELEK A., RANACHOWSKI Z., et al.: Effect of Al alloying on the Hall-Petch strengthening and AE in compressed Mg-Li-Al alloys before and after HPT processing. Kovove Materialy-Metallic Materials, 49, 4, 2011, 271–277.
- KUŚNIERZ J., PAWELEK A., RANACHOWSKI Z., et al.: Mechanical and Acoustic Emission Behaviour Induced by Channel-Die Compression of Mg-Li Nanocrystalline Alloys Obtained by ECAP Technique. Reviews on Advanced Materials Science, 18, 7, 2008, 583–589.
- RANACHOWSKI Z., RANACHOWSKI P., REJMUND F., et al.: The Study of Influence of High Pressure Torsion Process on Acoustic Emission Activity of Compressed Mg-Li Alloys. Archives of Acoustics, 33, 4, 2008, 123–128.
- RANACHOWSKI Z., BEJGER A.: Fault diagnostics of the fuel injection system of a medium power maritime diesel engine with application of acoustic signal. Archives of Acoustics, 30, 4, 2005, 465–472.
- BEJGER A.: Application of acoustic emission elastic waves for fuel systems testing of maritime Diesel engines (in Polish). Fotobit, Kraków 2012.